

$$\left. \begin{aligned}
 f(i,j) &= f(x_i, y_j) \\
 P(i,j) &= \sum_{l=1}^{\bar{N}} f(i,l) \bar{M}_j^{l-1} \\
 Q(i,j) &= \sum_{k=1}^N f(k,j) M_i^k \\
 R(i,j) &= \sum_{k=1}^N \sum_{l=1}^{\bar{N}} f(k,l) M_i^k \bar{M}_j^{l-1}
 \end{aligned} \right\} i = 1 \dots N, j = 1 \dots \bar{N} \quad (25.20)$$

For  $x < x_1$ ,  $x > x_N$ ,  $y < y_1$  or  $y > y_{\bar{N}}$  we extrapolate by using respectively  $S_{1,j}$ ,  $S_{N-1,j}$ ,  $S_{i,1}$ ,  $S_{i, \bar{N}-1}$ .

For one particular mesh the moments  $M_i^k$  and  $\bar{M}_j^{l-1}$  of the cardinal splines have to be computed only once. The three sets of quantities P, Q, R have to be calculated once for each function f to be interpolated. (In our calculations we have six such functions: the dimensionless force and torque components). To any point (x,y) belongs a rectangle characterized by the numbers i and j, and the eight quantities  $A_i$ ,  $B_i$ ,  $C_i$ ,  $D_i$ ,  $\bar{A}_j$ ,  $\bar{B}_j$ ,  $\bar{C}_j$ ,  $\bar{D}_j$  can be computed for that point. Then  $S(x,y)$  as given by (25.19) yields the interpolated value for the function f at (x,y).

## CHAPTER VI

### WIND TUNNEL EXPERIMENTS.

#### §26 *Boomerang arms in uniform straight flow.*

The main part of this chapter is concerned with experiments on rotating boomerangs. This section, however, deals with a preliminary experiment in which lift and drag coefficients of boomerang arms in a uniform, straight air flow were measured. Boomerang arms, i.e. the wings forming part of a boomerang, in free flight operate at Reynolds numbers of the order of  $10^5$  or less. In this region the wing characteristics may seriously deviate from those at the higher Reynolds numbers associated with ordinary aircraft (see e.g. [Schmitz, 1957], [Muesmann, 1959], [Kraemer, 1961a]).

To investigate this matter with respect to our boomerang arms measurements were carried out with a small wind tunnel at the Twente University of Technology. Its wind speed could be varied between 0 and 30 m/s. (Degree of turbulence unknown.) The measuring cross section was square, having sides of 45.7 cm (18"). Lift and drag of wings were measured by means of a three-component spring balance mounted in one side wall of the tunnel. One end of the wing was attached to the spring balance in such a way that the wing's spanwise direction was horizontal, perpendicular to the airflow and halfway between the tunnel's bottom and ceiling. Four wings were made each of which occupied the full tunnel width, so that a two-dimensional flow (expectedly) would result. In addition six boomerang arms were cut off from actual boomerangs (which were known to fly well), and used in the experiment.

Here only part of the data shall be presented, but enough to provide a fairly representative picture of the lift and drag of boomerang arms in uniform straight flow at  $Re \approx 4 \times 10^4$  to  $10^5$ . It should be emphasized that the measurements were not of high precision. More extensive and accurate information (but not on hand-made boomerang arms) can be found in [Lippisch, 1951], [Schmitz, 1957, 1954], [Muesmann, 1959], [Kraemer,

1961a]. The data presented here are taken from 24 (out of 64) measuring series, and concern three of the six boomerang arms and all four "two-dimensional" wings. Their cross sections are shown in fig. 26.1.

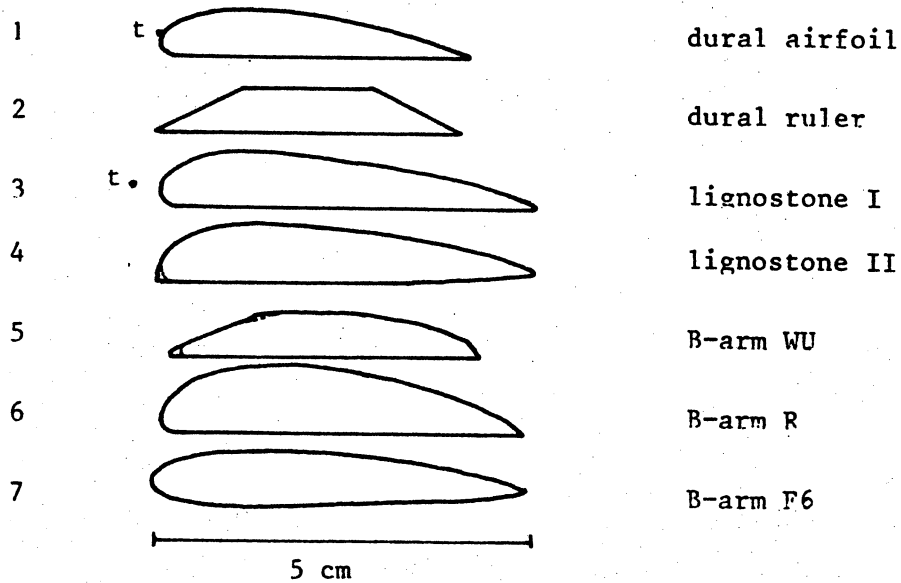


fig. 26.1. Cross sections of the wings used.

(t = turbulence wire,  $\curvearrowright$  rounding off, in part of the measurements.)

wing	length l	AR	chord c	thickn. t	t/c	remarks
1 dural airfoil	45.4	$\infty$	4.04	0.62	.154	also with turbulence wire
2 dural ruler	45.4	$\infty$	3.97	0.57	.144	
3 lignostone I	45.4	$\infty$	4.92	0.77	.157	also with turbulence wire
4 lignostone II	45.3	$\infty$	4.88	0.76	.156	also rounded
5 B-arm WU	28.6	15	3.86	0.61	.158	also rounded
6 B-arm R	26.6	12	4.7	0.94	.200	
7 B-arm F6	25.6	10	4.9	0.72	.147	

table 26.1. Some dimensions (cm) of the wings used.

Table 26.1 lists some of the dimensions of the wings used. Boomerang arms R and F6 are tapered, and for these the chord and thickness in the middle are listed. The aspect ratio for the arms is defined as:

$$AR = \frac{2l^2}{s} \quad (26.1)$$

where  $l$  = spanwise length,  $s$  = wing area. The factor 2 is due to the mirror effect of the tunnel wall. For the four "two-dimensional" wings we take  $AR = \infty$ . The Reynolds number is defined as:

$$Re = \frac{Vc}{\nu} \quad (26.2)$$

where  $V$  = air velocity,  $\nu$  = kinematic viscosity of air,  $c$  = chord length as listed in table 26.1. Theoretically an elliptic spanwise lift distribution would give rise to an induced drag coefficient (see e.g. [von Mises, 1959]):

$$C_D = \frac{C_L^2}{\pi AR} \quad (26.3)$$

The corresponding parabolic curves are drawn as thin lines in fig. 26.3A, B, C. Figures 26.2A, B, C, D and 26.3A, B, C show experimental polar curves i.e.  $C_D$ ,  $C_L$  graphs. The numbers in the graphs denote the angles of incidence, which, in this section, are the angles between the undisturbed airflow and the flat(test) part of the underside of the considered wing. Let us consider the experimental data wing for wing.

1. Dural airfoil: fig. 26.2A, fig. 26.3D.

This wing is milled from duraluminium. It has a smooth, airfoil-shaped profile. Similar wings were used in the experiments under water, described in §17 and §18. Comparison of the curve  $\circ$   $Re = 77000$  ( $V = 28.7$  m/s) with the curve  $\oplus$   $Re = 44000$  ( $V = 16.4$  m/s) shows the dependence on  $Re$  of both  $C_L$  and  $C_D$ . The favourable influence of a turbulence wire at  $Re = 44000$  ( $V = 16.4$  m/s) is evident from a comparison between the curves  $\oplus$  without wire and  $\blacktriangle$  with wire. The wire consisted of a piece of 0.05 cm thick cotton string glued to the wing's nose at both ends. Its position was influenced by the airflow, especially in the middle of the wing. As the wire touched the wing's nose it should be considered as a trip wire, see [Kraemer, 1961b]. Finally the curve  $\square$   $Re = 77000$  ( $V = 28.6$  m/s)

gives data for the reversed profile. Polar curves at  $Re = 81000$  (not shown) are essentially the same as those at  $Re = 77000$  (0, ○). Fig. 26.3D shows a remarkable hysteresis phenomenon.  $C_L$  and  $C_D$  are plotted as functions of  $Re$  (or  $V$ ) at a constant angle of incidence of  $5^\circ$ . For  $Re > 65000$ :  $C_L \approx 1.0$  and  $C_D \approx 0.05$ , whereas for  $Re < 53000$ :  $C_L \approx 0.5$  and  $C_D \approx 0.1$ . For  $53000 < Re < 65000$  the lift and drag coefficients depend on whether the situation was reached from the super- or from the subcritical state (see further down in this section).

### 2. Dural ruler: fig. 26.2C.

This wing was milled from duraluminium. It has a trapezium-shaped cross section with sharp edges, and front-rear symmetry. The trapezium's sharp angles equal  $27.4^\circ$ . The lift and drag characteristics are not significantly different at  $Re = 79000$  ( $V = 29.8$  m/s): 0 and  $Re = 44000$  ( $V = 16.5$  m/s): ⊕.  $C_D$  increases suddenly above  $7\frac{1}{2}^\circ$  angle of incidence, and again above  $15^\circ$ .

### 3. Lignostone I, fig. 26.2B.

This wing was hand-made from lignostone, a kind of impregnated, compressed beech ply. It has a flat underside. Its upper side was filed into shape and sanded smooth. The measurements were done without and with turbulence wire. In the latter case the wire consisted of a 0.05 cm (= 0.01 chord) thick piece of cotton string stretched in front of the wing's leading edge, parallel to it, at a distance of 0.3 cm (= 0.06 chord). The wire was fastened to the wing by means of two screws near the wing's ends. Without wire there is a slight dependence on  $Re$ : compare curve 0 at  $Re = 97000$  ( $V = 29.6$  m/s) with curve ⊕ at  $Re = 55000$  ( $V = 16.7$  m/s). With wire the  $Re$  dependence is restricted to angles of incidence higher than  $10^\circ$ : compare curve Δ at  $Re = 96000$  ( $V = 29.2$  m/s) with curve ▲ at  $Re = 54000$  ( $V = 16.3$  m/s). The influence of the turbulence wire is very pronounced: compare Δ with 0 resp. ▲ with ⊕. Stall is postponed by the wire from  $5^\circ$  to  $12\frac{1}{2}^\circ$  resp. from  $2\frac{1}{2}^\circ$  to  $10^\circ$ , and the maximum  $C_L$  is increased from 1.0 to 1.3 resp. from 0.8 to 1.2. At  $Re = 96000$  strong flutter occurred for angles of incidence near  $15^\circ$ . The curve ⊕ at  $Re = 55000$  ( $V = 16.7$  m/s) gives data for the reversed profile.

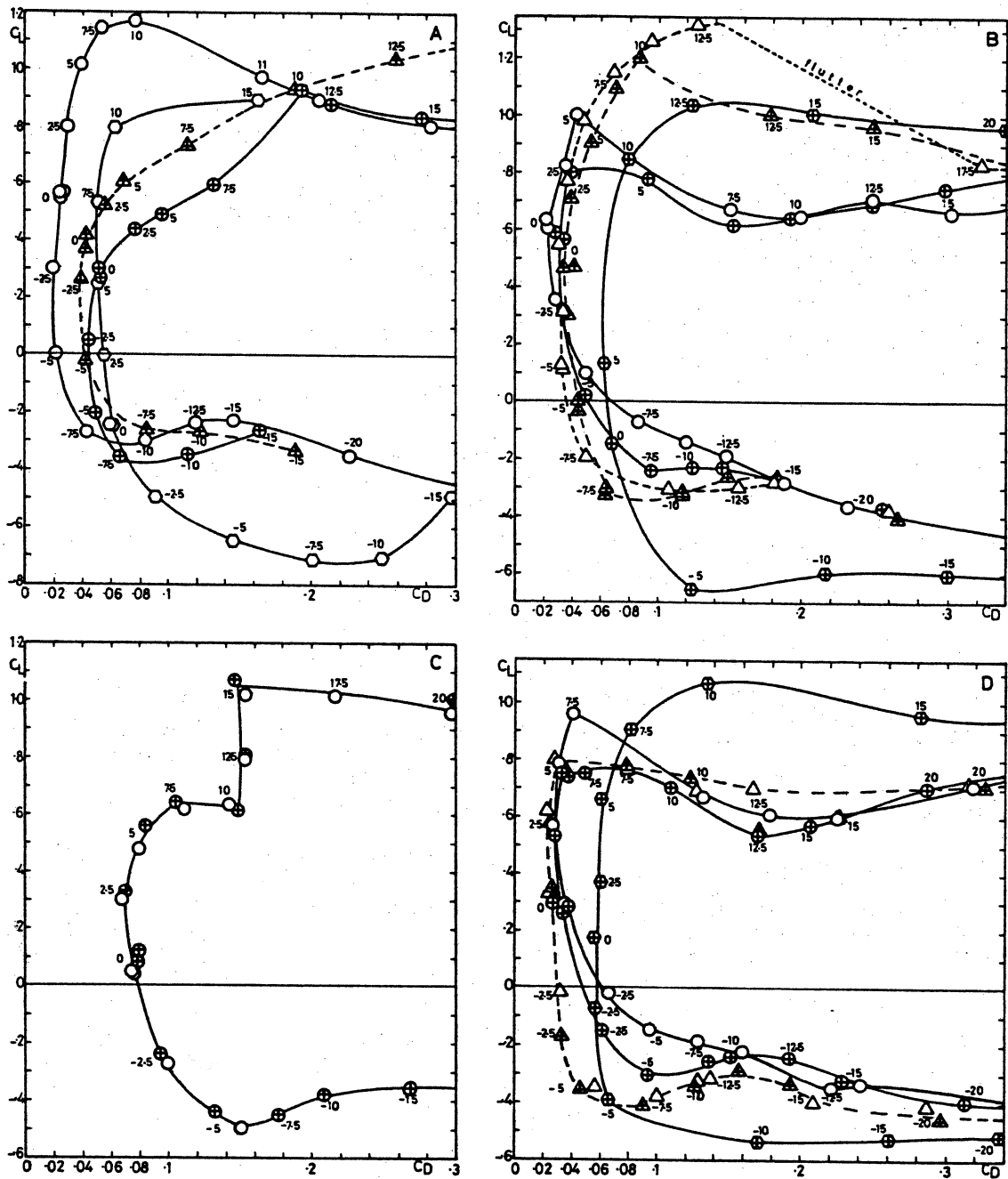


fig. 26.2. Experimental polar curves for 4 two-dimensional wings.  
 A. dural airfoil, O normal  $Re = 77000$ ,  $\odot$  normal  $Re = 44000$ ,  $\blacktriangle$  with turbulence wire  $Re = 44000$ ,  $\square$  reversed  $Re = 77000$ .  
 B. lignostone I, O normal  $Re = 97000$ ,  $\odot$  normal  $Re = 55000$ ,  $\triangle$  with turbulence wire  $Re = 96000$ ,  $\blacktriangle$  with turbulence wire  $Re = 54000$ ,  $\oplus$  reversed  $Re = 55000$ .  
 C. dural ruler, O  $Re = 79000$ ,  $\odot$   $Re = 44000$ .  
 D. lignostone II, O normal  $Re = 98000$ ,  $\odot$  normal  $Re = 53000$ ,  $\triangle$  rounded  $Re = 96000$ ,  $\blacktriangle$  rounded  $Re = 53000$ ,  $\oplus$  reversed  $Re = 53000$ .  
 Numbers with the experimental points denote the angles of incidence.